Determination of partonic energy loss from measured light charged particles and jets in PbPb collisions at LHC energies

Prashant Shukla[1,2†] **and Kapil Saraswat**[3,*]

[1]Nuclear Physics Division, Bhabha Atomic Research Center, Mumbai 400085, India.
[2]Homi Bhabha National Institute, Anushakti Nagar, Mumbai 400094, India.
[3]Department of Physics, DSB Campus, Kumaun University, Nainital - 263001, INDIA.

E-mail: † `pshuklabarc@gmail.com`

E-mail: * `kapilsaraswatbhu@gmail.com`

Abstract. We perform a comprehensive study of partonic energy loss reflected in the nuclear modification factors of charged particles and jets measured in PbPb collisions at $\sqrt{s_{\rm NN}}$ = 2.76 and 5.02 TeV in wide transverse momentum ($p_{\rm T}$) and centrality range. The $p_{\rm T}$ distributions in pp collisions are fitted with a modified power law and the nuclear modification factor in PbPb collisions can be obtained using effective shift ($\Delta p_{\rm T}$) in the spectrum measured at different centralities. Driven by physics consideration, the functional form of energy loss given by $\Delta p_{\rm T}$ can be assumed as power law with different power indices in three different $p_{\rm T}$ regions. The power indices and the boundaries of three $p_{\rm T}$ regions are obtained by fitting the measured nuclear modification factor as a function of $p_{\rm T}$ in all collision centralities simultaneously. The energy loss in different collisions centralities are best described by a square root dependence on number of participants. It is demanded that the three power law functions and their derivatives are continuous at the $p_{\rm T}$ boundaries. The energy loss for light charged particles is found to increase linearly with $p_{\rm T}$ in low $p_{\rm T}$ region below $\sim 5-6$ GeV/c and approaches a constant value in high $p_{\rm T}$ region above $\sim 22-29$ GeV/c with an intermediate power law connecting the two regions. The method is also used for jets and it is found that for jets, the energy loss increases approximately linearly even at very high $p_{\rm T}$ suggesting that their is no one-to-one correspondence between high $p_{\rm T}$ charged particle and high $p_{\rm T}$ jet.

1. Introduction

The collisions of heavy ions at ultra relativistic energies are performed to create and study bulk strongly interacting matter at high temperatures. The data from RHIC and LHC provide strong evidences of formation of a new state of matter known as quark gluon plasma (QGP) in these collisions [1]. The light charged hadrons and jets transverse momentum (p_{T}) spectra give insight into the particle production mechanism in pp collisions. The partonic energy energy loss is reflected in these particles when measured in heavy ion collisions due to jet-quenching [2] which measures the opacity of the medium. A modified power law distribution [3, 4, 5] describes the p_{T} spectra of the hadrons in pp collisions in terms of a power index n which determines the initial production in partonic collisions. In Ref.[6], the power law function is applied to heavy ion collisions as well which includes the transverse flow in low p_{T} region and the in-medium energy loss (also in terms of power law) in high p_{T} region.

The spectra of hadrons are measured in both pp and AA collisions and nuclear modification factor (R_{AA}) is obtained. The energy loss of partons can be understood as horizontal shift in the scaled hadron spectra in AA with respect to pp spectra as done by PHENIX measurement [7]. Their measurements of neutral pions upto $p_{\mathrm{T}} \sim 10$ GeV/c are consistent with the scenario where the momentum shift Δp_{T} is proportional to p_{T}. In similar approach, the authors in Ref. [8], extracted the fractional energy loss from the measured nuclear modification factor of hadrons as a function of p_{T} below 10 GeV/c in AuAu collisions at $\sqrt{s_{\mathrm{NN}}} = 200$ GeV. They also considered that the energy loss increases linearly with p_{T}. In recent PHENIX work [9], fractional energy loss was obtained in the hadron spectrum measured upto $p_{\mathrm{T}} = 20$ GeV/c in heavy ions collisions at RHIC and LHC energy and is not found to be constant. This means that a constant fractional energy loss (energy loss varying linearly with p_{T}) can be applicable only to low p_{T} RHIC measurements.

There are many recent studies which use so-called shift formalism to obtain the energy loss. The work in Ref.[10] is based on shift formalism and describes the transverse momentum (p_{T}), rapidity (y) and centrality dependences of the measured jet nuclear modification factor (R_{AA}) in PbPb collisions at LHC. They assume that the energy loss is given by a power law in terms of p_{T}, the value of power index is obtained between 0.4 to 0.8 by fitting the R_{AA} as a function of p_{T} and centralities. They also found that the energy loss linearly increases with number of participants. Using the same method they study the magnitude and the colour charge dependence of the energy loss in PbPb collisions at LHC energies using the measured data of the inclusive jet suppression [11]. The authors of the Ref.[12] work on inclusive charged particle spectra measured in the range ($5 < p_{\mathrm{T}} < 20$ GeV/c) in heavy ion collisions at RHIC and LHC. They assume that the energy loss linearly increases with p_{T} and pathlength.

There are detailed calculations of energy loss of partons in the hot medium [see e.g. Refs. [13, 14]. Phenomenoligical models tend to define simple dependence of the radiative energy loss of the parton on the energy of the parton inside the medium [for a discussions see Ref. [15]]. The energy loss can be characterized in terms of coherence length $l_{\rm coh}$, which is associated with the formation time of gluon radiation by a group of scattering centres. If $l_{\rm coh}$ is less then the mean free path (λ) of the parton, the energy loss is proportional to the energy of the parton. If $L_{\rm coh}$ is greater than λ but less than the path length (L) of the parton ($\lambda < l_{\rm coh} < L$), the energy loss is proportional to the square root of the energy of the parton. In the complete coherent regime, $L_{\rm coh} > L$, the energy loss is independent on energy but proportional to the path length. There is a nice description of charged particle spectra at RHIC using such a prescription by dividing the $p_{\rm T}$ spectra in three regions [16, 17].

In general, one can assume that the energy loss of partons in the hot medium as a function of parton energy is in the form of power law where the power index ranges from 0 (constant) to 1 (linear). Guided by these considerations, in the present work, the $p_{\rm T}$ loss has been assumed as power law with different power indices in three different $p_{\rm T}$ regions. The $p_{\rm T}$ distributions in pp collisions are fitted with a modified power law and $R_{\rm AA}$ in PbPb collisions can be obtained using effective shift ($\Delta p_{\rm T}$) in the $p_{\rm T}$ spectrum measured at different centralities. The power index and the boundaries of three $p_{\rm T}$ regions are obtained by fitting the measured $R_{\rm AA}$ of charged particles and jets in PbPb collisions at $\sqrt{s_{\rm NN}} = 2.76$ and 5.02 TeV in large transverse momentum ($p_{\rm T}$) and centrality range.

2. Nuclear Modification Factor and Energy Loss

The nuclear modification factor $R_{\rm AA}$ of hadrons is defined as the ratio of yield of the hadrons in AA collision and the yield in pp collision with a suitable normalization

$$R_{\rm AA}(p_{\rm T}, b) = \frac{1}{T_{\rm AA}} \frac{d^2N^{AA}(p_{\rm T}, b)}{dp_{\rm T}dy} / \frac{d^2\sigma^{pp}(p_{\rm T}, b)}{dp_{\rm T}dy} \ . \tag{1}$$

Here $T_{\rm AA}$ is the nuclear overlap function which can be calculated from the nuclear density distribution. High $p_{\rm T}$ partons traversing the medium loose energy and cause the suppression of hadrons at high $p_{\rm T}$ indicated by value of $R_{\rm AA}$ which is less than one. The transverse momentum distribution of hadrons in pp collisions can be described by the Hagedorn function which is a QCD-inspired summed power law [18] given as

$$\frac{d^2\sigma^{\rm pp}}{dp_{\rm T}dy} = A_n \ 2\pi p_{\rm T} \left(1 + \frac{p_{\rm T}}{p_0}\right)^{-n} . \tag{2}$$

where n is the power and A_n and p_0 are other parameters which are obtained by fitting the experimental pp spectrum. The yield in the AA collision can be obtained by shifting the spectrum by $\Delta p_{\rm T}$ as

$$\begin{aligned} \frac{1}{T_{\rm AA}} \frac{d^2N^{\rm AA}}{dp_{\rm T}dy} &= \frac{d^2\sigma^{\rm pp}(p'_{\rm T} = p_{\rm T} + \Delta p_{\rm T})}{dp'_{\rm T}dy} \frac{dp'_{\rm T}}{dp_{\rm T}} \\ &= \frac{d^2\sigma^{\rm pp}(p'_{\rm T})}{dp'_{\rm T}dy} \left(1 + \frac{d(\Delta p_{\rm T})}{dp_{\rm T}}\right) . \end{aligned} \tag{3}$$

The reasoning behind writing Eq. 3 lies in the assumption that particle yield at a given $p_{\rm T}$ in AA collisions would have been equal to the yield in pp collisions at $p_{\rm T} + \Delta p_{\rm T}$. The shift $\Delta p_{\rm T}$ includes the medium effect, mainly energy loss of parent quark inside the plasma.

The nuclear modification factor $R_{\rm AA}$ can be obtained as

$$R_{\rm AA} = \left(1 + \frac{\Delta p_{\rm T}}{p_0 + p_{\rm T}}\right)^{-n} \left(\frac{p_{\rm T} + \Delta p_{\rm T}}{p_{\rm T}}\right) \left(1 + \frac{d(\Delta p_{\rm T})}{dp_{\rm T}}\right) \tag{4}$$

The energy loss given by p_T loss, Δp_T can be extracted by fitting the experimental data on $R_{\rm AA}$ with Eq. 4. The $\Delta p_{\rm T}$ and its derivative will go as input in the above equation and can be assumed to be in the form of the power law with different values of power indices in three different $p_{\rm T}$ regions as follows

$$\Delta p_{\rm T} = \begin{cases} a_1 \, (p_{\rm T} - C_1)^{\alpha_1} & \text{for} \quad p_{\rm T} < p_{\rm T_1} \quad , \\ a_2 \, (p_{\rm T} - C_2)^{\alpha_2} & \text{for} \quad p_{\rm T_1} \leq p_{\rm T} < p_{\rm T_2} \quad , \\ a_3 \, (p_{\rm T} - C_3)^{\alpha_3} & \text{for} \quad p_{\rm T} \geq p_{\rm T_2} \ . \end{cases} \tag{5}$$

Here $a_1 = M\sqrt{N_{\rm part}/(2A)}$ is considered to be linearly dependent on the pathlength traversed by the parton given by square root of number of participants $N_{\rm part}$ in the collision. The parameter M relies on the energy density of the medium depending on the collision energy but has a same value for all centralities. The boundaries of the $p_{\rm T}$ regions $p_{\rm T_1}$, $p_{\rm T_2}$ and the power indices α_1, α_2 and α_3 in the three different regions are used as free parameters while fitting the $R_{\rm AA}$ measured at different centralities simultaneously. The parameter C_1 is fixed to a suitable value to choose a lower $p_{\rm T}$ cutoff and the parameters C_2, C_3, a_2 and a_3 are obtained by assuming the function and its derivative to be continuous at boundaries.

Demanding that the function in Eq. 5 to be continuous at $p_{\rm T} = p_{\rm T_1}$ and at $p_{\rm T} = p_{\rm T_2}$ we obtain

$$a_2 = a_1 \, \frac{(p_{\rm T_1} - C_1)^{\alpha_1}}{(p_{\rm T_1} - C_2)^{\alpha_2}} \quad . \tag{6}$$

$$a_3 = a_2 \, \frac{(p_{\rm T_2} - C_2)^{\alpha_2}}{(p_{\rm T_2} - C_3)^{\alpha_3}} \quad . \tag{7}$$

Demanding that at $p_{\rm T} = p_{\rm T_1}$, the derivative of Eq. 5 is continuous.

$$a_1 \, \alpha_1 \, (p_{\rm T_1} - C_1)^{(\alpha_1 - 1)} = a_2 \, \alpha_2 \, (p_{\rm T_1} - C_2)^{(\alpha_2 - 1)} \quad , \tag{8}$$

Using the value of a_2 from Eq. 6

$$\frac{\alpha_1}{(p_{\rm T_1} - C_1)} = \frac{\alpha_2}{(p_{\rm T_1} - C_2)} \quad , \tag{9}$$

$$C_2 = p_{\rm T_1} - \frac{\alpha_2}{\alpha_1}(p_{\rm T_1} - C_1) \ . \tag{10}$$

Similarly, demanding the derivative to be continuous at $p_{\rm T} = p_{\rm T_2}$, we get C_3

$$C_3 = p_{\rm T_2} - \frac{\alpha_3}{\alpha_2}(p_{\rm T_2} - C_2) \ . \tag{11}$$

3. Results and Discussions

Figure 1 shows the invariant yields of the charged particles as a function of the transverse momentum p_T for pp collisions at $\sqrt{s} = 2.76$ TeV measured by the CMS experiment [19]. The solid curve is the Hagedorn distribution fitted to the p_T spectra with the parameters given in Table 1.

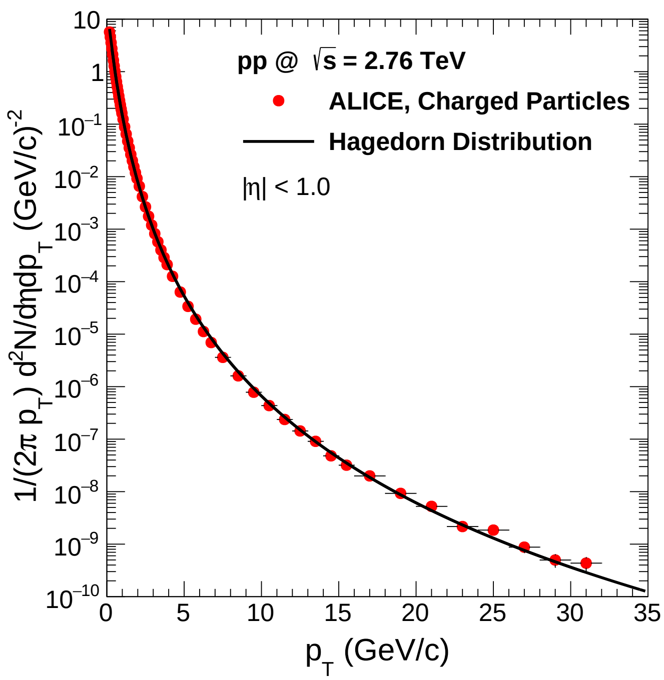

Figure 1. The invariant yields of the charged particles as a function of transverse momentum p_T for pp collision at $\sqrt{s} = 2.76$ TeV measured by the CMS experiment [19]. The solid curve is the fitted Hagedorn function.

Table 1. Parameters for the Hagedorn function obtained by fitting the transverse momentum spectra of charged particles and jets measured in pp collisions at $\sqrt{s_\mathrm{NN}} =$ 2.76 and 5.02 TeV.

Parameters	Charged particles		Jets	
	$\sqrt{s_\mathrm{NN}} = 2.76$ TeV	$\sqrt{s_\mathrm{NN}} = 5.02$ TeV	$\sqrt{s_\mathrm{NN}} = 2.76$ TeV	$\sqrt{s_\mathrm{NN}} = 5.02$ TeV
n	7.26 ± 0.08	6.70 ± 0.14	7.28 ± 2.0	7.42 ± 1.22
p_0 (GeV/c)	1.02 ± 0.04	0.86 ± 0.16	22.60 ± 3.6	36.45 ± 4.0
χ^2/NDF	0.15	0.06	0.23	0.95

Figure 2 shows the nuclear modification factor R_AA of the charged particles as a function of the transverse momentum p_T for different centrality classes in PbPb collisions at $\sqrt{s_\mathrm{NN}} = 2.76$ TeV measured by the CMS experiment [19]. The solid lines are the function given by Eq. 4. The modelling of centrality dependence with $\sqrt{N_\mathrm{part}}$ gives a good description of the data. The extracted parameters of the energy loss obtained by fitting the R_{AA} measured in different centrality classes of PbPb collisions at $\sqrt{s_{\mathrm{NN}}}$ = 2.76 TeV are given in Table 2 along with value of χ^2/NDF. It shows that the Δp_{T} increases almost linearly ($p_{\mathrm{T}}^{0.975}$) upto $p_{\mathrm{T}} \simeq 5$ GeV/c in confirmation with earlier studies. After that it increases slowly with power $\alpha = 0.224$ upto a p_{T} value 29 GeV/c and then becomes constant for higher values of p_{T}.

Table 2. The extracted parameters of the energy loss obtained by fitting the charged particles R_{AA} measured in different centrality classes of PbPb collisions at $\sqrt{s_{\mathrm{NN}}}$ = 2.76 and 5.02 TeV.

Parameters	$\sqrt{s_{\mathrm{NN}}} = 2.76$ TeV	$\sqrt{s_{\mathrm{NN}}} = 5.02$ TeV
M	0.705 ± 0.15	0.771 ± 0.036
p_{T_1} (GeV/c)	5.03 ± 0.15	5.12 ± 0.20
p_{T_2} (GeV/c)	29.0 ± 0.18	22.6 ± 5.7
C_1 (GeV/c)	1.0 (fixed)	1.0
α_1	0.975 ± 0.020	0.96 ± 0.04
α_2	0.224 ± 0.020	0.22 ± 0.03
α_3	0.05 ± 0.14	0.05 ± 0.10
$\frac{\chi^2}{\mathrm{NDF}}$	0.33	0.37

Figure 3 shows the energy loss Δp_{T} of the charged particles as a function of the transverse momentum p_{T} for different centrality classes in PbPb collision at $\sqrt{s_{\mathrm{NN}}}$ = 2.76 TeV. The Δp_{T} is obtained from Eq. 5 with parameters given in Table 2. The Δp_{T} increases from peripheral to the most central collision regions as per $\sqrt{N_{\mathrm{part}}}$. The figure shows that the Δp_{T} increases almost linearly upto $p_{\mathrm{T}} \sim 5$ GeV/c. After that it increases slowly upto a p_{T} value 29 GeV/c and then becomes constant for higher values of p_{T}.

Figure 4 shows the invariant yields of the charged particles as a function of the transverse momentum p_{T} for pp collisions at $\sqrt{s} = 5.02$ TeV measured by the CMS experiment [20]. The solid lines are the Hagedorn function fitted to the measured p_{T} spectra the parameters of which are given in Table 1.

Figure 5 shows the nuclear modification factor R_{AA} of the charged particles as a function of the transverse momentum p_{T} for different centrality classes in PbPb collisions at $\sqrt{s_{\mathrm{NN}}} = 5.02$ TeV measured by the CMS experiment [20]. The solid curves are the R_{AA} fitting function (Eq. 4). Here also the modelling of centrality dependence with $\sqrt{N_{\mathrm{part}}}$ gives a good description of the data. The extracted parameters of the energy loss obtained by fitting the R_{AA} measured in different centrality classes of PbPb collisions at $\sqrt{s_{\mathrm{NN}}} = 5.02$ TeV are given in Table 2 along with the value of χ^2/NDF. It shows that the Δp_{T} increases almost linearly ($p_{\mathrm{T}}^{0.96}$) similar to the case at 2.76 TeV for p_{T} upto 5 GeV/c. After that it increases slowly with power $\alpha = 0.22$ upto a p_{T} value 22 GeV/c and then becomes constant for higher values of p_{T} right upto 160 GeV/c.

Figure 6 shows the energy loss Δp_{T} of the charged particles as a function of the transverse momentum p_{T} for different centrality classes in PbPb collision at $\sqrt{s_{\mathrm{NN}}}$ =

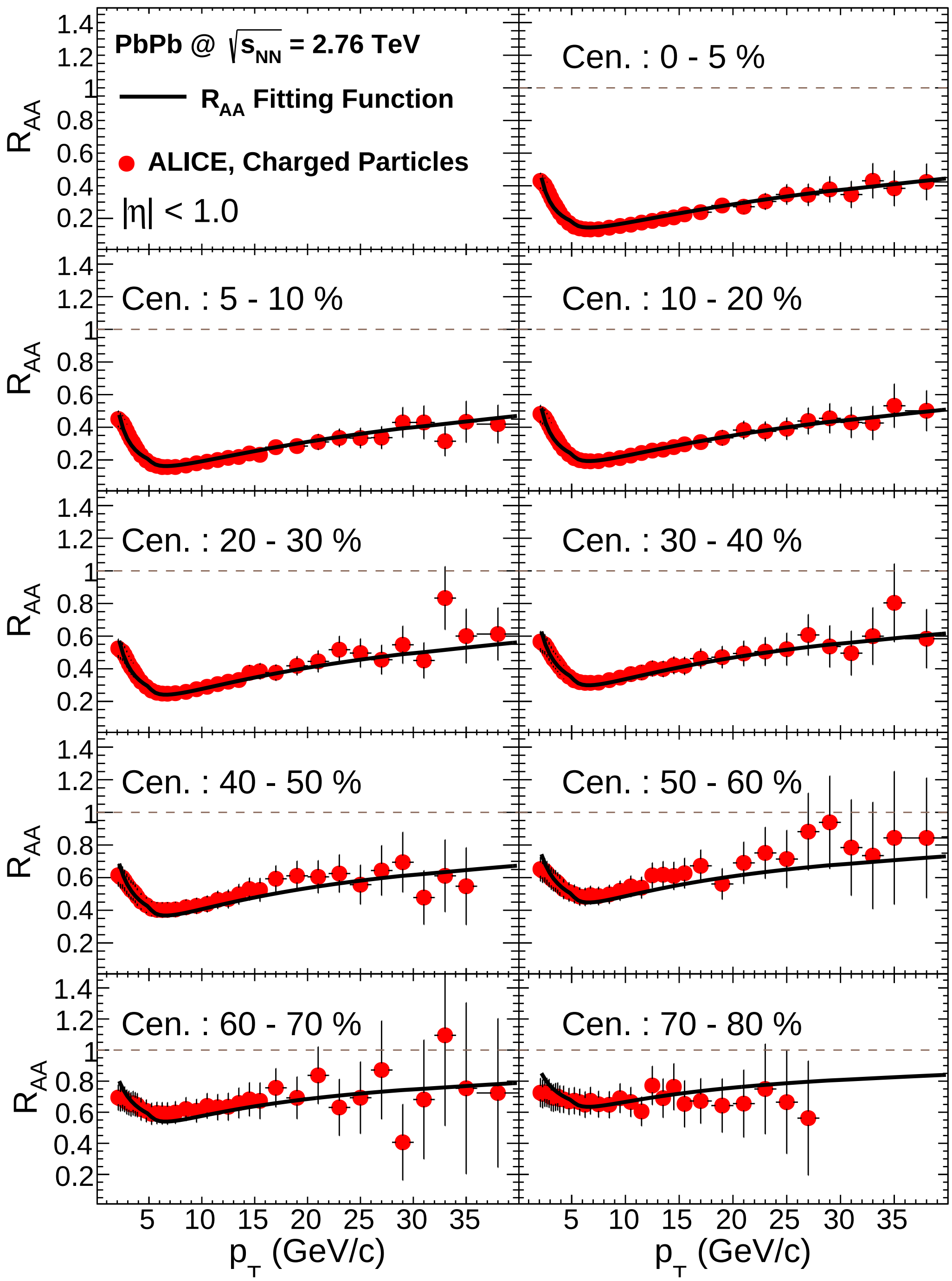

Figure 2. The nuclear modification factor $R_{\rm AA}$ of the charged particles as a function of transverse momentum $p_{\rm T}$ for various centrality classes in PbPb collisions at $\sqrt{s_{\rm NN}} =$ 2.76 TeV measured by the CMS experiment [19]. The solid curves are the $R_{\rm AA}$ fitting function (Eq. 4).

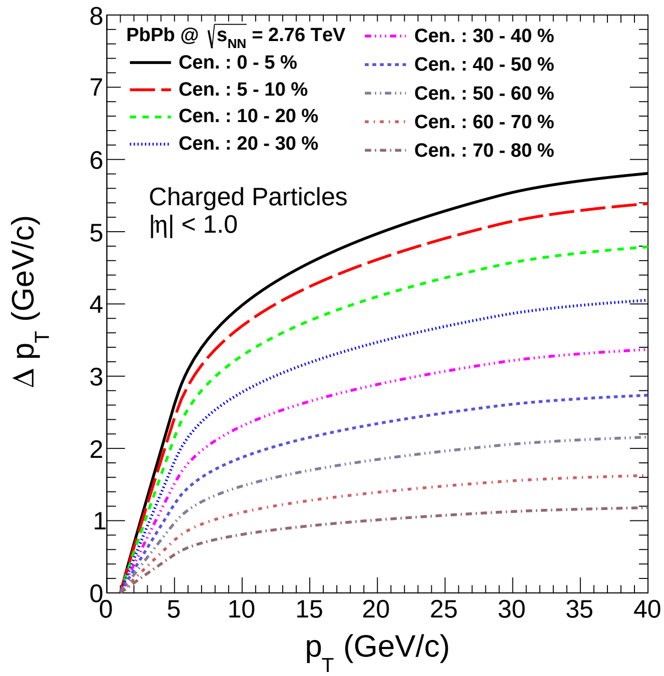

Figure 3. The energy loss Δp_{T} of the charged particles as a function of transverse momentum p_{T} in PbPb collision at $\sqrt{s_{\mathrm{NN}}} = 2.76$ TeV for different centrality classes.

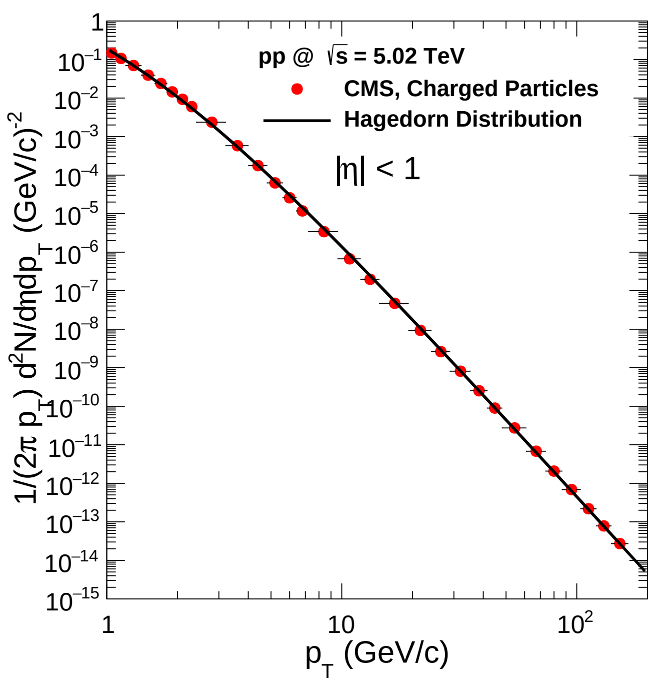

Figure 4. The invariant yields of the charged particles as a function of transverse momentum p_{T} for pp collision at $\sqrt{s} = 5.02$ TeV measured by the CMS experiment [20]. The solid curve is the fitted Hagedorn function.

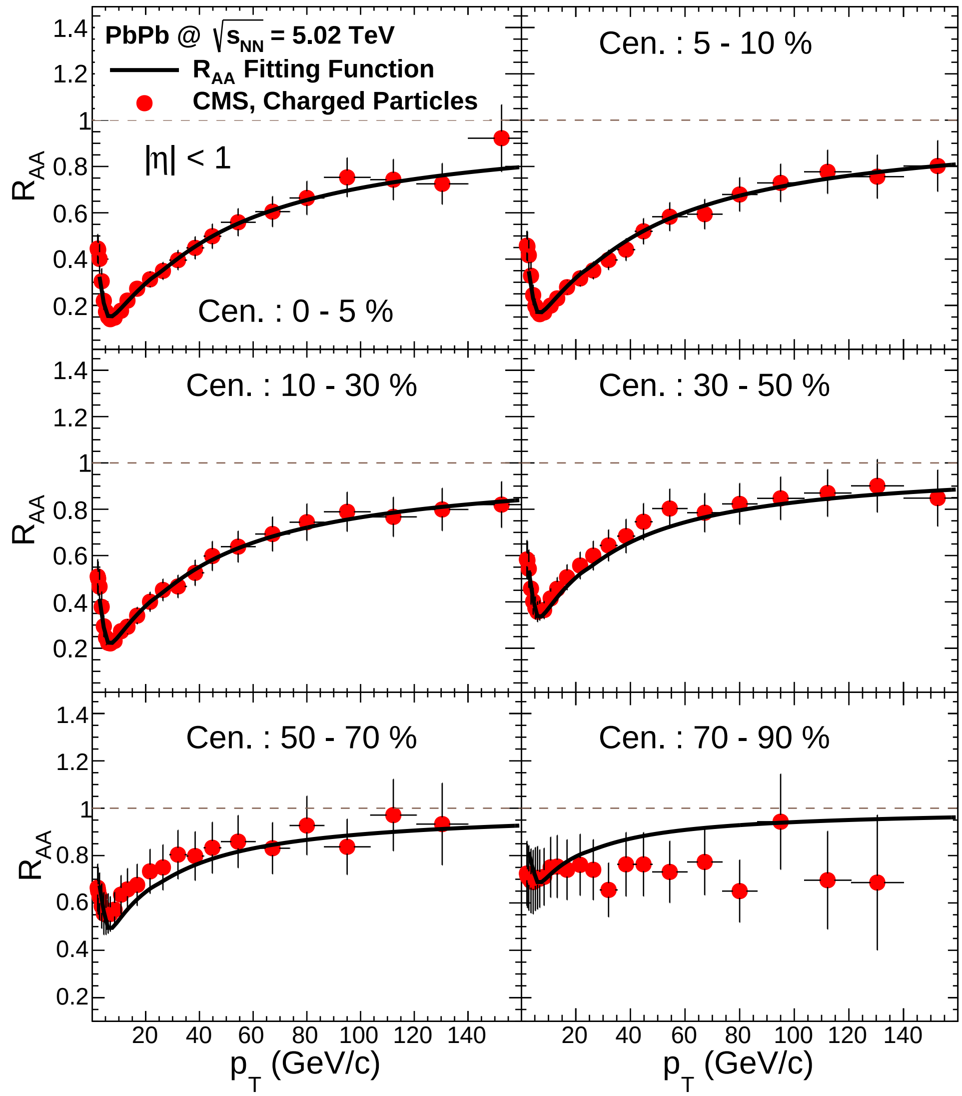

Figure 5. The nuclear modification factor $R_{\rm AA}$ of the charged particles as a function of transverse momentum $p_{\rm T}$ for various centrality classes in PbPb collisions at $\sqrt{s_{\rm NN}}$ = 5.02 TeV measured by the CMS experiment [20]. The solid lines are the $R_{\rm AA}$ fitting function (Eq. 4).

5.02 TeV. The $\Delta p_{\rm T}$ is obtained from Eq. 5 with the parameters given in Table 2. The $\Delta p_{\rm T}$ becomes constant from $p_{\rm T}$ starting from 22 GeV/c to 160 GeV/c and increases as the collisions become more central as per $\sqrt{N_{\rm part}}$.

Figure 7 shows the energy loss $\Delta p_{\rm T}$ of the charged particles as a function of the transverse momentum $p_{\rm T}$ for 0 - 5 % centrality class in PbPb collision at $\sqrt{s_{\rm NN}}$ = 2.76 and 5.02 TeV. The $\Delta p_{\rm T}$ at 5.02 TeV is similar but slightly more than that at 2.76 TeV.

Figure 8 shows the invariant yields of the jets as a function of the transverse momentum $p_{\rm T}$ for pp collisions at $\sqrt{s}$ = 2.76 TeV measured by the ATLAS experiment[21]. The solid curve is the Hagedorn distribution fitted to the $p_{\rm T}$ spectra, the parameters of which are given in Table 1.

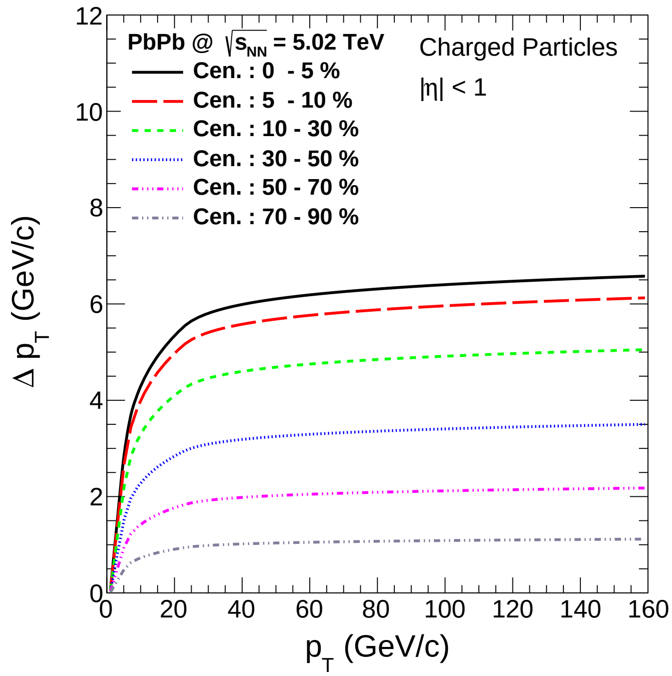

Figure 6. The energy loss Δp_{T} of the charged particles as a function of transverse momentum p_{T} in PbPb collision at $\sqrt{s_{\mathrm{NN}}} = 5.02$ TeV for different centrality classes.

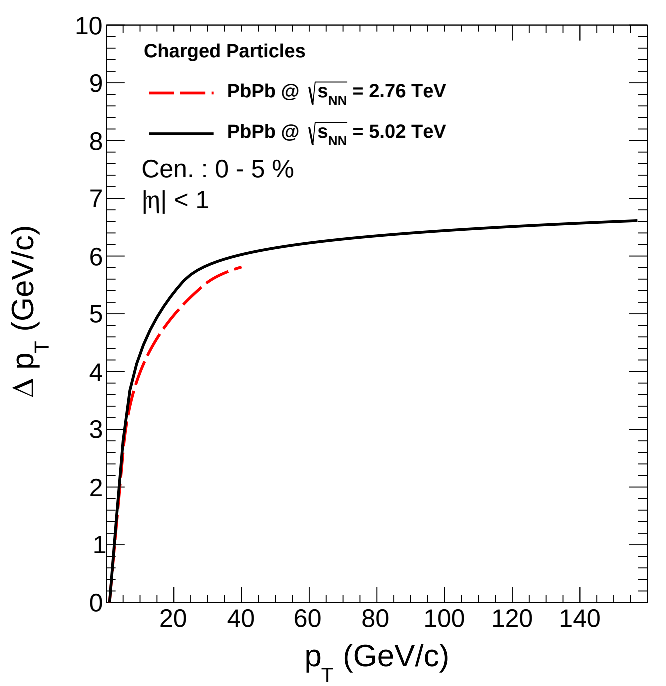

Figure 7. The energy loss Δp_{T} of the charged particles as a function of transverse momentum p_{T} in PbPb collision at $\sqrt{s_{\mathrm{NN}}} = 2.76$ and 5.02 TeV for 0 - 5 % centrality.

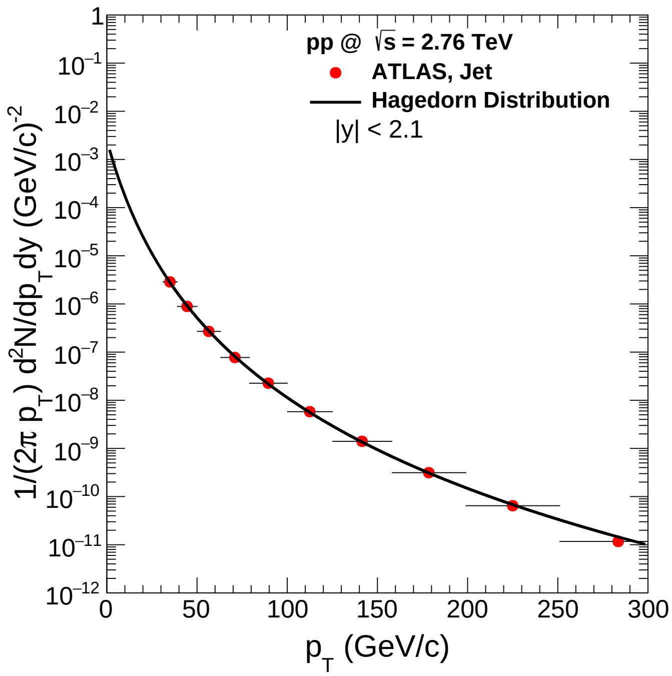

Figure 8. The invariant yields of the jets as a function of transverse momentum $p_{\rm T}$ for pp collision at $\sqrt{s} = 2.76$ TeV measured by the ATLAS experiment [21]. The solid curve is the fitted Hagedorn distribution.

Figure 9 shows the nuclear modification factor $R_{\rm AA}$ of the jets as a function of the transverse momentum $p_{\rm T}$ for different centrality classes in PbPb collisions at $\sqrt{s_{\rm NN}} =$ 2.76 TeV measured by the ATLAS experiment [21]. The solid curves are the $R_{\rm AA}$ fitting function (Eq. 4). Here also the modelling of centrality dependence with $\sqrt{N_{\rm part}}$ gives a good description of the data. The extracted parameters of the energy loss obtained by fitting the $R_{\rm AA}$ measured in different centrality classes of PbPb collisions at $\sqrt{s_{\rm NN}} =$ 2.76 TeV are given in Table 3 along with the value of χ^2/NDF. It shows that the $\Delta p_{\rm T}$ increases as $p_{\rm T}^{0.73}$ at all the values of $p_{\rm T}$ measured for jets.

Table 3. The extracted parameters of the energy loss obtained by fitting the jet $R_{\rm AA}$ measured in different centrality classes of PbPb collisions at $\sqrt{s_{\rm NN}} = 2.76$ and 5.02 TeV.

Parameters	$\sqrt{s_{\rm NN}} = 2.76$ TeV	$\sqrt{s_{\rm NN}} = 5.02$ TeV
M	0.43 ± 0.18	0.40 ± 0.10
C (GeV/c)	-54.4 ± 22.5	-128 ± 15
α	0.735 ± 0.08	0.73 ± 0.01
$\frac{\chi^2}{\rm NDF}$	0.27	0.95

Figure 10 shows the energy loss $\Delta p_{\rm T}$ of the jets as a function of the transverse momentum $p_{\rm T}$ for different centrality classes in PbPb collision at $\sqrt{s_{\rm NN}} = 2.76$ TeV.

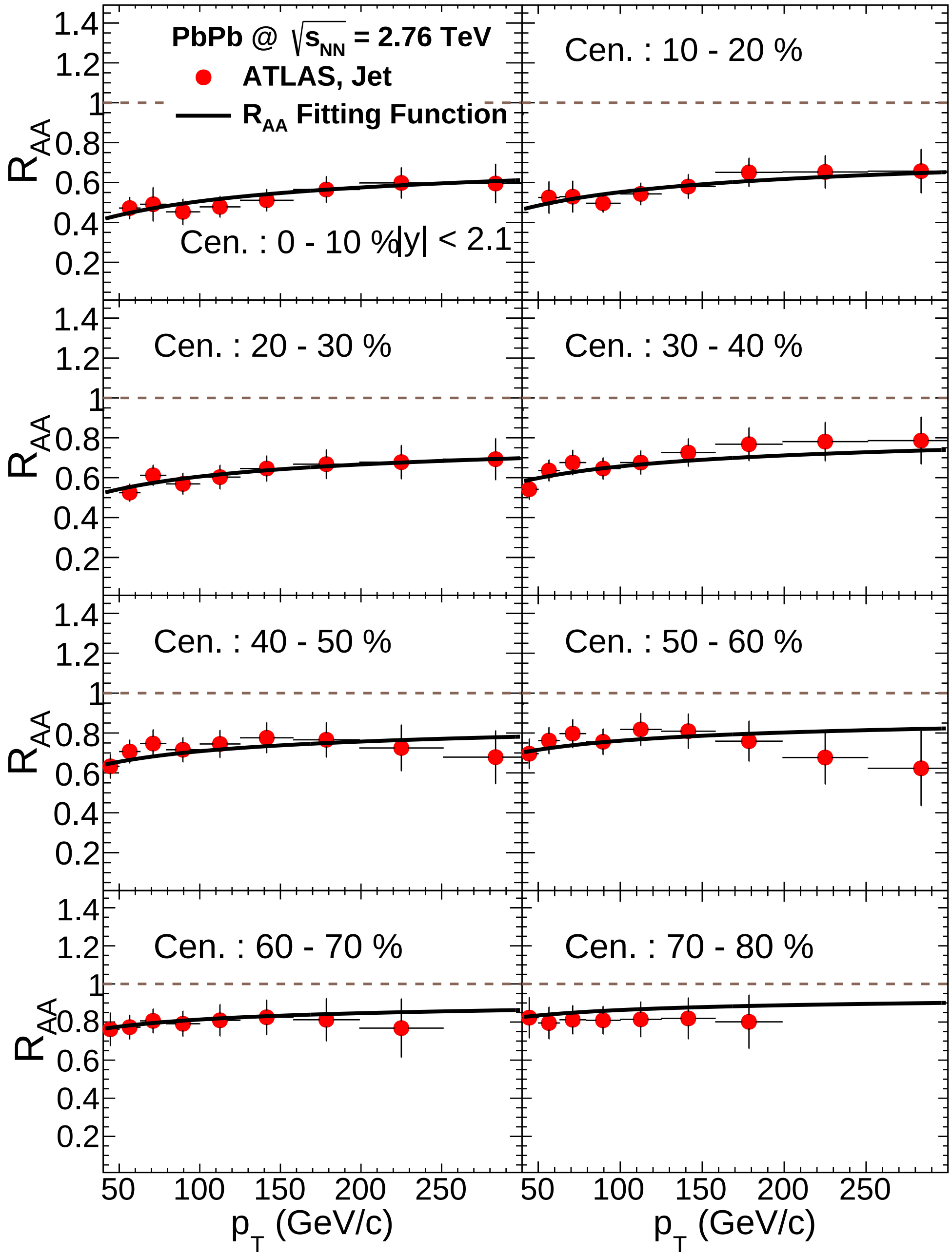

Figure 9. The nuclear modification factor R_{AA} of jets as a function of transverse momentum p_{T} for various centrality classes in PbPb collisions at $\sqrt{s_{\mathrm{NN}}} = 2.76$ TeV measured by the ATLAS experiment [21]. The solid curves are the R_{AA} fitting function given by Eq. 4.

The $\Delta p_{\rm T}$ is obtained from Eq. 5 using the parameters given in Table 3. The $\Delta p_{\rm T}$ increases from peripheral to the most central collision regions. The figure shows that the $\Delta p_{\rm T}$ increases almost linearly at all the values of $p_{\rm T}$ measured for jets.

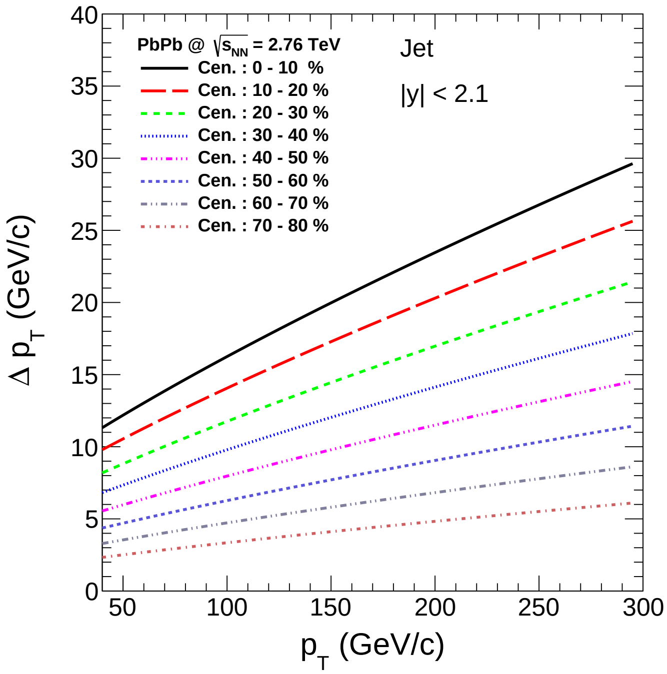

Figure 10. The energy loss $\Delta p_{\rm T}$ of the jet as a function of transverse momentum $p_{\rm T}$ in PbPb collision at $\sqrt{s_{\rm NN}} = 2.76$ TeV for different centrality classes.

Figure 11 shows the invariant yields of the jets as a function of the transverse momentum $p_{\rm T}$ for pp collisions at $\sqrt{s} = 5.02$ TeV measured by the ATLAS experiment [22]. The solid curve is the Hagedorn distribution with the parameters given in Table 1.

Figure 12 shows the nuclear modification factor $R_{\rm AA}$ of the jets as a function of the transverse momentum $p_{\rm T}$ for different centrality classes in PbPb collisions at $\sqrt{s_{\rm NN}} = 5.02$ TeV measured by the ATLAS experiment [22]. The solid curves are the $R_{\rm AA}$ fitting function (Eq. 4). Here also the modelling of centrality dependence with $\sqrt{N_{\rm part}}$ gives a good description of the data. The extracted parameters of the energy loss obtained by fitting the $R_{\rm AA}$ measured in different centrality classes of PbPb collisions at $\sqrt{s_{\rm NN}} = 5.02$ TeV are given in Table 3, along with the value of χ^2/NDF. It shows that the $\Delta p_{\rm T}$ increases as $p_{\rm T}^{0.73}$ at all the values of $p_{\rm T}$ measured for jets similar to the case of jets at $\sqrt{s_{\rm NN}} = 5.02$ TeV

Figure 13 shows the energy loss $\Delta p_{\rm T}$ of the jets as a function of the transverse momentum $p_{\rm T}$ for different centrality classes in PbPb collision at $\sqrt{s_{\rm NN}} = 5.02$ TeV. The $\Delta p_{\rm T}$ is obtained from Eq. 5 with the parameters given in Table 3. The $\Delta p_{\rm T}$ increases from peripheral to the most central collision regions. The figure shows that the $\Delta p_{\rm T}$ increases almost linearly at all the values of $p_{\rm T}$ measured for jets.

Figure 14 shows the energy loss $\Delta p_{\rm T}$ of the jets as a function of the transverse momentum $p_{\rm T}$ in the most central (0-10%) PbPb collision at $\sqrt{s_{\rm NN}} = 2.76$ and 5.02

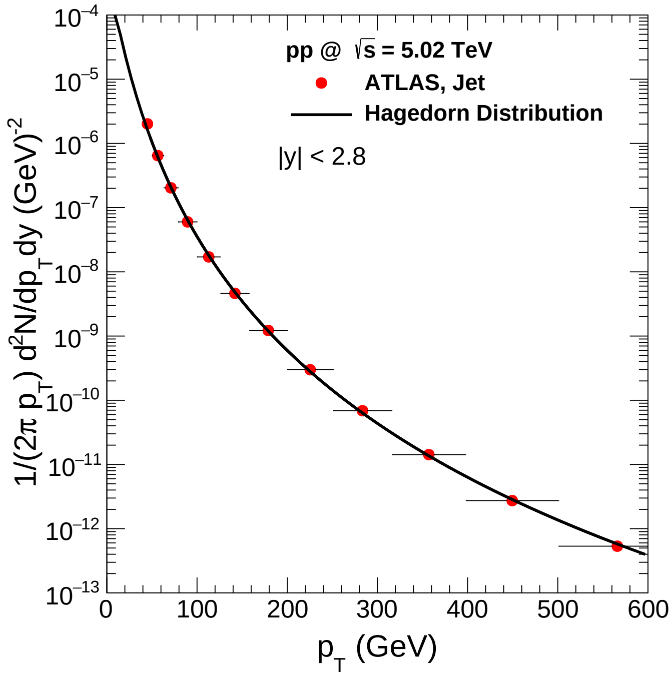

Figure 11. The invariant yields of the jets as a function of transverse momentum $p_{\rm T}$ for pp collision at $\sqrt{s} = 5.02$ TeV measured by the ATLAS experiment [22]. The solid curve is the fitted Hagedorn distribution.

TeV. These are compared with the $\Delta p_{\rm T}$ obtained for charged particles in the 0-5% centrality class of PbPb collision at $\sqrt{s_{\rm NN}} = 5.02$ TeV. The energy loss $\Delta p_{\rm T}$ in case of jets for both the energies increases with $p_{\rm T}$. The values of $\Delta p_{\rm T}$ at 5.02 TeV is more than that at 2.76 TeV. This behaviour at high $p_{\rm T}$ is very different from the energy loss of charged particles which becomes constant in these $p_{\rm T}$ regions.

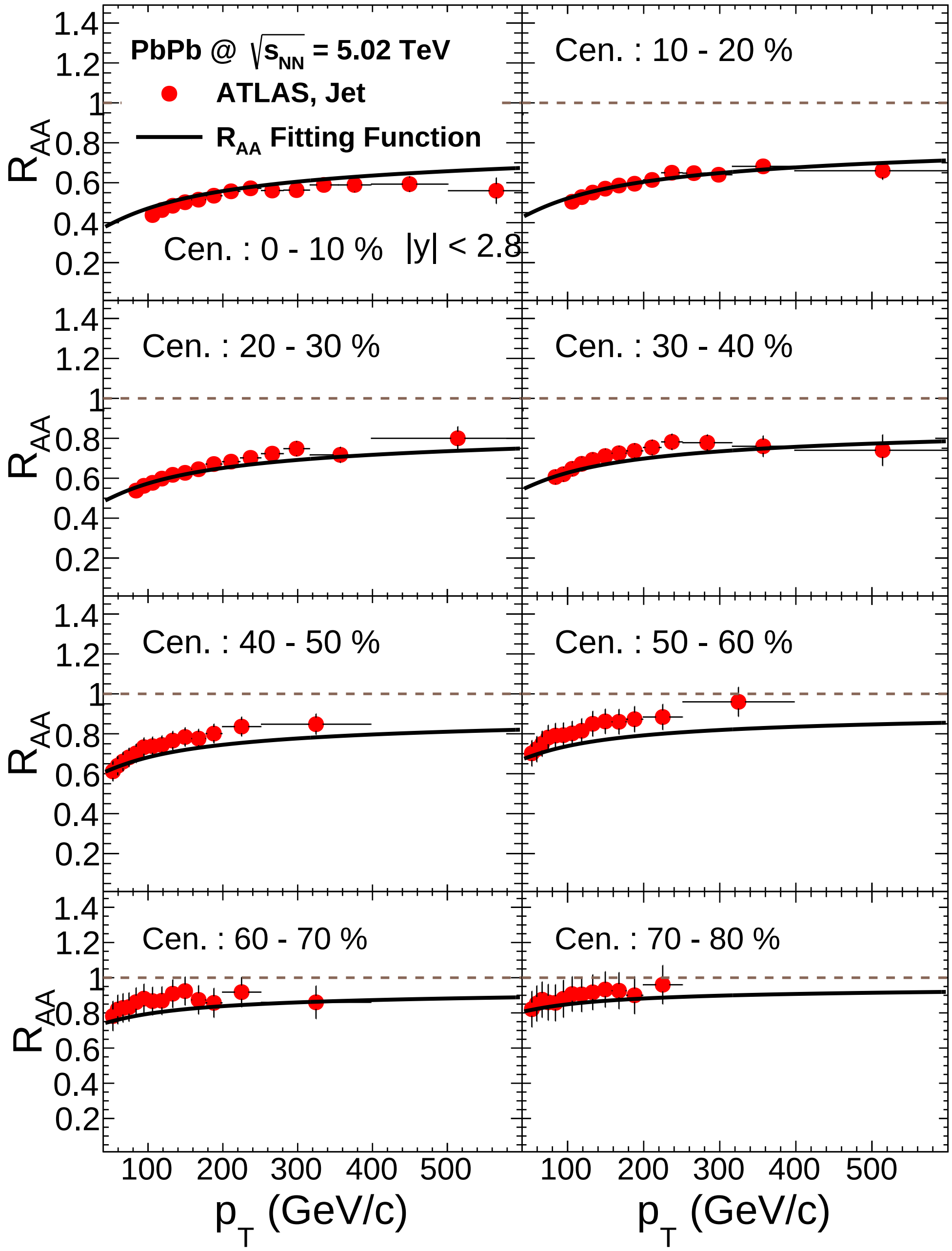

Figure 12. The nuclear modification factor R_{AA} of the jets as a function of transverse momentum p_{T} for various centrality classes in PbPb collisions at $\sqrt{s_{\mathrm{NN}}} = 5.02$ TeV measured by the ATLAS experiment [22]. The solid curves are the R_{AA} fitting function given by Eq. 4.

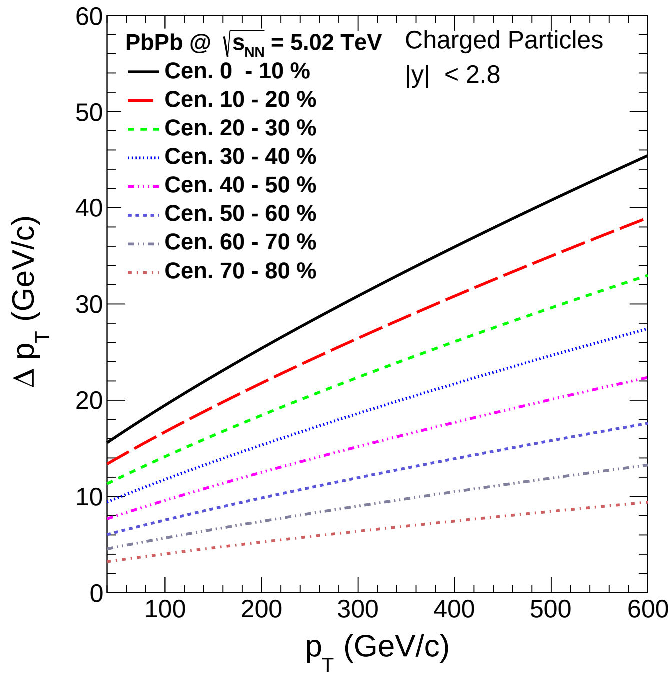

Figure 13. The energy loss $\Delta p_{\rm T}$ of the jet as a function of transverse momentum $p_{\rm T}$ in PbPb collision at $\sqrt{s_{\rm NN}} = 5.02$ TeV for different centrality classes.

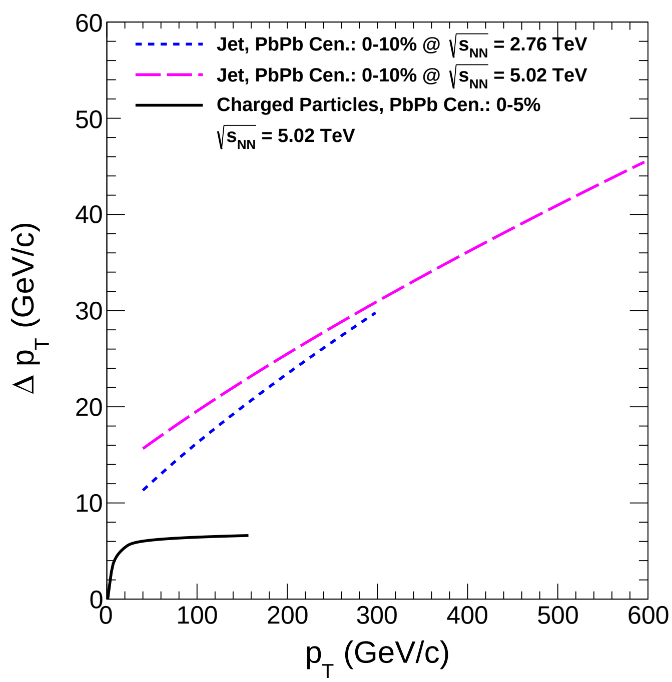

Figure 14. The energy loss $\Delta p_{\rm T}$ of the jets as a function of transverse momentum $p_{\rm T}$ in the most central PbPb collision at $\sqrt{s_{\rm NN}} = 2.76$ and 5.02 TeV. The $\Delta p_{\rm T}$ obtained for charged particles in the most central PbPb collision at $\sqrt{s_{\rm NN}} = 5.02$ TeV is also shown.

4. Conclusions

We presented a study of partonic energy loss extracted from the measured $R_{\rm AA}$ of charged particles and jets in PbPb collisions at $\sqrt{s_{\rm NN}}$ 2.76 and 5.02 TeV in wide transverse momentum and centrality range. The functional form of energy loss given by $\Delta p_{\rm T}$ has been assumed as power law with different power indices in three different $p_{\rm T}$ regions driven by physics considerations. The power indices and the boundaries of three $p_{\rm T}$ regions are obtained by fitting the experimental data of $R_{\rm AA}$ as a function of $p_{\rm T}$ and centrality. The modelling of centrality dependence with $\sqrt{N_{\rm part}}$ gives a good description of the data. The energy loss for light charged particles is found to increase linearly with $p_{\rm T}$ in low $p_{\rm T}$ region below 5-6 GeV/c and approaches a constant value in high $p_{\rm T}$ region above 25 GeV/c with an intermediate power law connecting the two regions. The $\Delta p_{\rm T}$ at 5.02 TeV is similar but slightly more than that at 2.76 TeV. The method is also used for jets and it is found that for jets, the energy loss increases almost linearly even at very high $p_{\rm T}$ suggesting that there is no one-to-one correspondence between high $p_{\rm T}$ charged particle and high $p_{\rm T}$ jet.

References

[1] F. Antinori, A. Dainese, P. Giubellino, V. Greco, M. P. Lombardo and E. Scomparin, Nucl. Phys. A **982** (2019) pp.1-1066.
[2] X. N. Wang, Phys. Lett. B **579** (2004) 299, [nucl-th/0307036].
[3] C. Tsallis, J. Statist. Phys. **52** (1988) 479.
[4] T. S. Biro, G. Purcsel and K. Urmossy, Eur. Phys. J. A **40** (2009) 325, [arXiv:0812.2104 [hep-ph]].
[5] P. K. Khandai, P. Sett, P. Shukla and V. Singh, Int. J. Mod. Phys. A **28** (2013) 1350066, [arXiv:1304.6224 [hep-ph]].
[6] K. Saraswat, P. Shukla and V. Singh, J. Phys. Comm. **2** (2018) no.3, 035003, [arXiv:1706.04860 [hep-ph]].
[7] S. S. Adler *et al.* [PHENIX Collaboration], Phys. Rev. C **76** (2007) 034904. [nucl-ex/0611007].
[8] G. Wang and H. Z. Huang, Phys. Lett. B **672** (2009) 30, [arXiv:0810.2822 [nucl-ex]].
[9] A. Adare *et al.* [PHENIX Collaboration], Phys. Rev. C **93** (2016) no.2, 024911. [arXiv:1509.06735 [nucl-ex]].
[10] M. Spousta and B. Cole, Eur. Phys. J. C **76** (2016) no.2, 50, [arXiv:1504.05169 [hep-ph]].
[11] M. Spousta, Phys. Lett. B **767** (2017) 10, [arXiv:1606.00903 [hep-ph]].
[12] A. Ortiz and O. Vazquez, Phys. Rev. C **97** (2018) no.1, 014910, [arXiv:1708.07571 [hep-ph]].
[13] X. N. Wang, M. Gyulassy and M. Plumer, Phys. Rev. D **51** (1995) 3436, [hep-ph/9408344].
[14] R. Baier, Y. L. Dokshitzer, A. H. Mueller, S. Peigne and D. Schiff, Nucl. Phys. B **483** (1997) 291, [hep-ph/9607355].
[15] R. Baier, D. Schiff and B. G. Zakharov, Ann. Rev. Nucl. Part. Sci. **50** (2000) 37, [hep-ph/0002198].
[16] S. De and D. K. Srivastava, J. Phys. G **39** (2012) 015001, Erratum: [J. Phys. G **40** (2013) 049502], [arXiv:1107.5659 [nucl-th]].
[17] S. De and D. K. Srivastava, J. Phys. G **40** (2013) 075106, [arXiv:1112.2492 [nucl-th]].
[18] R. Hagedorn, Riv. Nuovo Cim. **6N10** (1983) 1 .
[19] A. S. Yoon [CMS Collaboration], arXiv:1107.1862 [nucl-ex].
[20] V. Khachatryan *et al.* [CMS Collaboration], JHEP **1704**, 039 (2017), CMS-HIN-15-015, CERN-EP-2016-242, [arXiv:1611.01664 [nucl-ex]].

[21] G. Aad *et al.* [ATLAS Collaboration], Phys. Rev. Lett. **114** (2015) 072302 , CERN-PH-EP-2014-172, [arXiv:1411.2357 [hep-ex]].

[22] M. Aaboud *et al.* [ATLAS Collaboration], CERN-EP-2018-105, arXiv:1805.05635 [nucl-ex].